plants

MDPI

Article

Effect of Carbon and Nitrogen Addition on $\delta^{13}C$ and $\delta^{18}O$ Values of CO_2 Released from Soil Collars Under Forest and Lawn Across Seasons

Xingkai Xu [1,2,*], Yuhua Kong [3], Jin Yue [4], Weiguo Cheng [5], Vladimir Shanin [6], Dmitriy Khoroshaev [6] and Irina Kurganova [6]

1 State Key Laboratory of Atmospheric Environment and Extreme Meteorology, Institute of Atmospheric Physics, Chinese Academy of Sciences, Beijing 100029, China
2 Department of Atmospheric Chemistry and Environmental Science, College of Earth and Planetary Sciences, University of Chinese Academy of Sciences, Beijing 100049, China
3 College of Forestry, Henan Agricultural University, Zhengzhou 450046, China; y.kong@henau.edu.cn
4 Sub-Center for Atmospheric Research in Ecosystem Networks, Institute of Atmospheric Physics, Chinese Academy of Sciences, Beijing 100029, China; yuejin@mail.iap.ac.cn
5 Faculty of Agriculture, Yamagata University, Tsuruoka 997-8555, Japan; cheng@tds1.tr.yamagata-u.ac.jp
6 V.A. Kovda Institute of Physicochemical and Biological Problems in Soil Science of the Russian Academy of Sciences, Pushchino 142290, Russia; shaninvn@gmail.com (V.S.); d.khoroshaev@pbcras.ru (D.K.); ikurg@mail.ru (I.K.)
* Correspondence: xingkai_xu@mail.iap.ac.cn

Abstract

A full-season soil-core experiment examined how carbon (C) and nitrogen (N) additions, alone and combined, affect $\delta^{13}C$ and $\delta^{18}O$ of soil-respired CO_2 under forest and lawn, and how these isotopes relate to soil CH_4 flux, non-substrate-derived CO_2 emission, temperature, and moisture. Carbon addition alone (sucrose) enriched $\delta^{13}C$ and depleted $\delta^{18}O$ under both vegetation types, whereas N addition alone (ammonium chloride) had no detectable effect. The N + C treatment caused stronger isotopic changes than N alone but did not differ significantly from C alone, suggesting that N modulates C-induced isotopic fractionation rather than acting independently. Forest soils had lower mean $\delta^{13}C$ and $\delta^{18}O$ than lawn soils; both isotopes peaked in autumn and were lowest in summer. $\delta^{18}O$ decreased nonlinearly with increasing CH_4 uptake and non-substrate-derived CO_2 emission, but these processes explained little of the variation in $\delta^{13}C$. Soil moisture dominated $\delta^{13}C$, where soil temperature dominated $\delta^{18}O$. Overall, $\delta^{13}C$ mainly traces carbon sources and microbial decomposition, whereas $\delta^{18}O$ is more sensitive to thermal–hydrological regimes and gas exchange. The two isotopes are therefore complementary for understanding soil respiration and improving terrestrial C-cycle models. Vegetation type and season were key regulators, and future work should include soil-water $\delta^{18}O$ measurements, separation of root and microbial respiration, and longer-term observations across diverse climatic regions.

Keywords: carbon dioxide; $\delta^{13}C$; $\delta^{18}O$; methane; nutrient addition; soil respiration; vegetation type; seasonal variation

Check for updates

Academic Editor: Emilia Fernández Ondoño

Received: 27 September 2026
Revised: 11 November 2026
Accepted: 17 November 2026
Published: 28 November 2026

Copyright: © 2026 by the authors. Licensee MDPI, Basel, Switzerland. This article is an open access article distributed under the terms and conditions of the Creative Commons Attribution (CC BY) license.

1. Introduction

Soil respiration is one of the largest terrestrial fluxes of carbon dioxide (CO_2) to the atmosphere, releasing roughly ten times the CO_2 emitted annually by global fossil fuel combustion [1]. It comprises autotrophic respiration from plant roots and heterotrophic respiration driven by soil microorganisms decomposing organic matter. The two components

respond differently to exogenous carbon (C) and nitrogen (N) inputs, and the direction and magnitude of these responses depend on ecosystem type, the duration and dose of N input, and soil C availability and pH [2–7]. Given the increasing global extent of N deposition, a central scientific issue in global change ecology is how exogenous C and N additions modulate both the rate and source partitioning of soil respiration [7–9].

Stable carbon ($\delta^{13}C$) and oxygen ($\delta^{18}O$) isotopes serve as powerful "natural fingerprint" tools for disentangling these sources [10–14] because photosynthesis and respiration exert opposing effects on the $\delta^{13}C$ and $\delta^{18}O$ signatures of atmospheric CO_2 [15–17]. CO_2 from distinct sources carries a characteristic isotopic imprint: in forest ecosystems, the $\delta^{13}C$ of CO_2 derived from soil organic matter decomposition ($\delta^{13}C$-CO_2) is typically 2–4‰ higher than that of root and associated microbial respiration [12,18]. This difference has made $\delta^{13}C$ a widely used tracer for partitioning soil respiration and ecosystem respiration [11,13,19]. Oxygen isotopes offer complementary insight. The $\delta^{18}O$ of soil-respired CO_2 ($\delta^{18}O$-CO_2) primarily reflects full isotopic equilibrium with soil water at depths of 5–15 cm and is related to soil carbonic anhydrase activity [20–22]. Moreover, because soil-water $\delta^{18}O$ varies seasonally with precipitation, evaporation, and plant water uptake, $\delta^{18}O$-CO_2 can effectively trace soil moisture conditions and dynamic CO_2 sources [10,14,17,22–25]. Since $\delta^{13}C$ traces carbon source and microbial decomposition, whereas $\delta^{18}O$ traces soil biophysical conditions and gas transport, comparing the two isotopes can reveal whether C and N additions act mainly on substrate use or on the soil biophysical environment.

Whether C and N additions leave detectable and mechanistically interpretable isotopic imprints, however, remains unresolved. Three issues persist in the literature. First, the direction of the isotopic response is uncertain because microbial responses are method-dependent. Nitrogen addition generally suppresses soil respiration and enhances soil organic C storage [26,27], but its effect on microbial C use efficiency (CUE) differs between approaches: the ^{13}C-substrate method indicates an approximately 12% decrease, whereas the ^{18}O-H_2O method suggests an approximately 11% increase [28]. This discrepancy matters because CUE governs whether added C is respired or retained, and thus whether the $\delta^{13}C$ of respired CO_2 shifts. Consistent with this, long-term N addition experiments with $\delta^{13}C$-CO_2 measurements show that microbes in fertilized soils shift their primary C source from native soil organic C to plant litter under warming [29]. Ground covers such as moss can further modify soil microenvironments and substrate utilization [30], and the response of soil respiration to N input also depends on soil C availability [7]. Second, the relative strength of vegetation type versus season as controls on these isotopic imprints is unclear. Grasslands release relatively "young" CO_2 ($^{14}CO_2$ close to modern atmospheric values), whereas forest soils include contributions from decades-old organic matter [31]; C_4 plants can further enrich the $\delta^{13}C$ of respired CO_2 in grasslands [32]. Soil texture, organic matter content, and carbonic anhydrase activity also affect C turnover and the isotopic composition of soil respiration [22,33,34]. Seasonally, $\delta^{13}C$-CO_2 tends to be higher in summer and lower in winter and spring [13,35], while $\delta^{18}O$-CO_2 shows ^{18}O enrichment in winter when soils are water-saturated [20,36,37]. These patterns reflect shifts in root versus microbial contributions [18,38], respiratory substrates [35], and soil hydrothermal conditions [30,34,36,39]. Moisture-induced isotopic variation has been documented in forests and grasslands, including a negative correlation between soil $\delta^{13}C$-CO_2 and moisture [40], a parabolic relationship between ecosystem respiration $\delta^{13}C$ and mean annual precipitation [41], and more depleted $\delta^{18}O$ of respired CO_2 in wet than in dry seasons [42]. These studies, however, largely ignored C and N additions and rarely compared land-use types. Third, whether the C × N interaction is additive or non-additive relative to the single additions has not been tested. Direct investigations of C addition alone remain scarce; hence, the interactive regulation of C and N on $\delta^{13}C$-CO_2 and $\delta^{18}O$-CO_2 is poorly understood.

These three issues motivate three hypotheses. First, if the two isotopes are governed by different mechanisms, δ^{13}C-CO_2 should be mediated jointly by substrate availability, N-induced shifts in substrate use and pH, and CH_4-derived CO_2. In contrast, δ^{18}O-CO_2 should respond primarily to soil moisture and temperature conditions (H1). Methane uptake in the forest floor is constrained by N addition and the resulting low pH [6,43–46], and natural biogenic CH_4 sources have an average δ^{13}C value of approximately –63.0‰ [47]. Therefore, CO_2 from CH_4 oxidation may partly contribute to the δ^{13}C of CO_2 accumulated during opaque chamber closure. Consequently, C addition should shift the two isotopes in opposite directions, whereas N addition should exert a comparatively weak effect on both. Second, if vegetation type and season differ in their control strength, the δ^{13}C-CO_2 response should be stronger in forest than in lawn. This expectation reflects the larger pool of older, ^{13}C-enriched organic matter in forest, whereas the δ^{18}O-CO_2 response should differ mainly through contrasts in soil texture, moisture, and gas transport. If season modulates treatment effects more strongly than vegetation type, δ^{13}C-CO_2 should respond most strongly in the warm, moist growing season, while δ^{18}O-CO_2 should track soil moisture and gas transport rather than treatment (H2). Third, if C and N act on different substrates or pathways, their combination should produce divergent effects on δ^{13}C-CO_2 and δ^{18}O-CO_2, and the C × N interaction may be non-additive relative to the single additions (H3).

To test hypotheses H1–H3, we conducted an *in situ* soil-core experiment under a temperate forest and adjacent lawn at the Changbai Mountain Forest Ecosystem National Research Station. The experiment included four treatments: C addition (sucrose), N addition (ammonium chloride), combined N + C addition, and a control. Across three seasons of the vegetation growing period, we measured δ^{13}C and δ^{18}O values of soil-respired CO_2, together with associated non-substrate-derived CO_2 emission and CH_4 flux, soil moisture, and soil temperature. Our objectives were: (1) to elucidate how C addition, N addition, and their combination affect the isotope composition of soil-respired CO_2 and to identify the key underlying mechanisms; (2) to compare the differential isotopic responses between forest and lawn ecosystems; and (3) to reveal the seasonal dynamics of these effects. By addressing these objectives, this study will deepen understanding of how C and N inputs regulate soil C cycling and provide isotope-based insights for predicting soil C dynamics in diverse terrestrial ecosystems under increasing N deposition and enhanced C input via rising atmospheric CO_2 concentrations and litter management.

2. Materials and Methods

2.1. Study Site and Soil Properties

The experiment was conducted under a forest and an adjacent lawn at the National Research Station of Changbai Mountain Forest Ecosystems (42°24′ N and 128°6′ E), located at the foot of the Changbai Mountains in northeastern China. The forest stand is dominated by mountain poplar (*Populus davidiana* Dode) and Korean pine (*Pinus koraiensis* Sieb. et Zucc.). The dominated trees are over 40 years old, with sparse moss cover and few Korean pine seedlings on the forest floor. The stand has a 2–3 cm thick organic layer and an A horizon approximately 6 cm deep. The adjacent lawn is dominated by *Trifolium repens* L., *Chelidonium majus* L., *Poa pratensis* L., *Capsella bursa-pastoris* (L.) Medik., *Ranunculus repens* L., *Eleusine indic* (L.) *Gaertn*., and *Digitaria sanguinalis* (L.) Scop. Most lawn grasses are perennial grasses typical of cold-temperate regions. The lawn also has an A horizon approximately 6 cm depth and is fertilized and mowed annually.

Over the past two decades, mean annual temperature and precipitation have been approximately 4.1 °C and 770 mm, respectively, with more than 80% of the rainfall occurring from May to October. Both the temperate forest and lawn soils are classified as Andosols and were artificially mixed with sand during station construction. Total organic C and total

N contents were 44.1 g C kg^{-1} and 2.2 g N kg^{-1} in the forest soil, and 63.8 g C kg^{-1} and 3.0 g N kg^{-1} in the lawn soil. For surface soil (0–10 cm depth), bulk density and alkaline-hydrolyzable N content were 1.0 g cm^{-3} and 186.1 µg N g^{-1} under forest, and 1.1 g cm^{-3} and 223.8 µg N g^{-1} under lawn. According to the official USDA Soil Texture Triangle (accessed at https://solvebility.com/soil_texture_classifier_professional_calculator/ accessed on 11 November 2026), the forest soil is loamy sand, whereas the lawn soil is sandy loam. Soil particle size was measured using a Mastersizer 2000 (Malvern, UK), with sandy, silt, and clay contents of 81.0%, 11.1%, and 7.9% in the forest soil and 73.8%, 12.6%, and 13.6% in the lawn soil, respectively.

2.2. Layout of the In Situ Soil-Core Experiment

For each seasonal field measurement campaign, three independent study plots (approximately 4 m × 4 m each) were randomly established in the forest and lawn. Within each plot, four soil cores were randomly assigned to four treatments: control, carbon (C) addition, nitrogen (N) addition, and combined N + C addition. Each core was enclosed by a rigid UPVC (unplasticized polyvinyl chloride) collar (20 cm in diameter and 20 cm in height) inserted 10 cm into the soil. This setup allowed us to monitor the $\delta^{13}C$ and $\delta^{18}O$ values of CO_2 released from soil respiration, together with soil CO_2 and CH_4 fluxes, temperature, and moisture (Figure 1). Positioning the collars to a depth of approximately 10 cm under forest and lawn reduced root damage and helped keep the cores in place. Field measurements were conducted in summer and autumn 2025 and spring 2026. Using these *in situ* soil-core experiments, we examined how the isotopic composition of soil-respired CO_2 responded to exogenous C, N, and their combination under forest and lawn. By integrating soil moisture, temperature, and greenhouse gas flux data, we further explored the response patterns and underlying mechanisms driving isotopic variations across seasons and vegetation types.

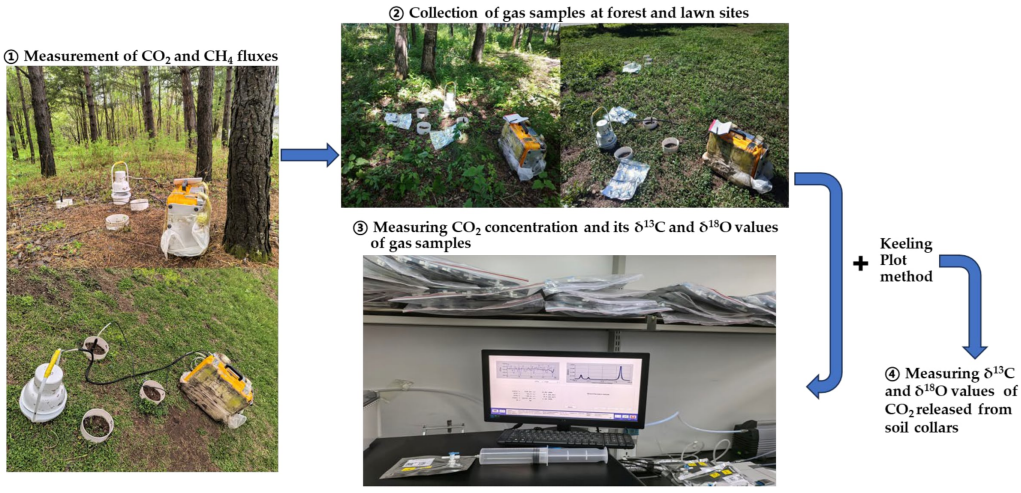

Figure 1. Apparatus for measuring CO_2 and CH_4 fluxes and the $\delta^{13}C$ and $\delta^{18}O$ values of CO_2 released from soil collars under forest and lawn. Before each flux measurement, grasses and litter inside the collars were removed.

To better simulate realistic scenarios of multiple C and N inputs (e.g., root exudates, litter decomposition, and artificial N input) and their effects on the isotope signatures of soil-respired CO_2 under field conditions, two successive rounds of C and/or N additions were performed during each seasonal measurement campaign. The second addition was applied only after soil CO_2 emissions had nearly stabilized following the first addition. This stabilization corresponded to 30–50% and 10–40% of the flux peak under forest and lawn, respectively. After each addition, *in situ* measurements of $\delta^{13}C$ and $\delta^{18}O$ values in

soil-respired CO_2, CO_2 and CH_4 fluxes, and soil temperature and moisture were conducted at regular intervals. Nitrogen was applied as ammonium chloride at a rate of 4.5 g N m^{-2} per event, equivalent to twice the annual dissolved total N input via natural throughfall in the local forest. Carbon was supplied as sucrose at a rate of 6.4 g C m^{-2} per event, corresponding to twice the water-soluble C content in local forest floor litter [48]. Both C and N amendments were dissolved in pure water and sprayed evenly on the soil cores before each seasonal measurement campaign, while control plots received an equal amount (150 mL) of pure water only. Because the $\delta^{13}C$ value of the added sucrose is –12‰, the CO_2 emission derived from non-substrate decomposition in C-amended soils, with and without N co-addition, was calculated using the isotopic mixing models described in Section 2.4. This calculation allowed us to assess whether the observed seasonal isotopic values of soil-respired CO_2 are linked to non-substrate-derived CO_2 emission under forest and lawn.

2.3. Measurements of $\delta^{13}C$ and $\delta^{18}O$ Values in Soil-Respired CO_2 and of CO_2 and CH_4 Fluxes

Frequent field observations of the isotopic composition of soil-respired CO_2 and associated auxiliary variables were conducted under forest and lawn over three seasons (summer 2025, autumn 2025, and spring 2026). In each season, two successive rounds of C and N additions were applied. The first addition was followed by measurements at predetermined intervals. The second addition was performed only after intermittent measurements confirmed that soil CO_2 emission had stabilized and corresponded to 30–50% and 10–40% of the flux peak under forest and lawn, respectively. The sampling schedules were as follows:

- Summer 2025: after the first addition, measurements at 0.5, 17, and 41 h; second addition at 71h, followed by measurements at 0.5, 4, 19, 43, and 72 h.
- Autumn 2025: after the first addition, measurements at 0.5, 3, 20, and 44 h; second addition at 139 h, followed by measurements at 0.5, 5, 29, and 53.5 h.
- Spring 2026: after the first addition, measurements at 0.5, 4, 20, and 44 h; second addition at 139 h, followed by measurements at 0.5, 4, 20, and 92 h.

Gas samples for isotopic analysis were collected using a static chamber method, with air-tight 100-mL syringes and 300-mL air-tight gas bags (NDEV41-0.3, Dalian Delin Gas Packing Co., Ltd., Dalian, China) at regular closure intervals (e.g., 0, 5, and 10 min, depending on CO_2 flux intensity, to minimize disturbance of the soil-atmosphere system in the collars) (Figure 1) [49]. Before each isotopic measurement, CO_2 and CH_4 fluxes from the soil collars, together with soil temperature and moisture, were monitored using a portable greenhouse gas analyzer (915-0011, Los Research Inc., Fremont, CA, USA) coupled to an opaque smart respiratory chamber (SC-11, Beijing LICA United Technology Limited, Beijing, China) (Figure 1) [50].

Within one week of headspace sampling, CO_2 concentration and its $\delta^{13}C$ and $\delta^{18}O$ values in each gas bag were determined using a CO_2 isotope spectrum analyzer (CCIA-38d-EP, Los Research Inc., Fremont, CA, USA) with a manual injection model (Figure 1). The $\delta^{13}C$ and $\delta^{18}O$ values of CO_2 were calculated relative to the Pee Dee Belemnite standard using Equation (1):

$$\delta^{13}C \text{ or } \delta^{18}O\ (‰) = (R_{sample}/R_{standard} - 1) \times 1000 \quad (1)$$

where $\delta^{13}C$ and $\delta^{18}O$ denote $\delta^{13}C$ and $\delta^{18}O$ values of CO_2, respectively. $R_{standard}$ and R_{sample} denote the molar ratios of $^{13}C/^{12}C$ (or $^{18}O/^{16}O$) in the standard and sample, respectively.

Before each analytical run, the CO_2 isotope analyzer was calibrated using two certified CO_2 standard mixtures of different concentrations, each containing 1% Argon (w/w) and balance air. The CO_2 concentrations and their $\delta^{13}C$ and $\delta^{18}O$ values were: 398.60 µL L^{-1}, −22.31‰, and −31.00‰; and 794.30 µL L^{-1}, −22.34‰, and −31.20‰. The source of these

standards, the measurement procedures, and the analytical precision of the CCIA-38d-EP analyzer have been detailed by Xu et al. [39]. For each measurement event, both $\delta^{13}C$ and $\delta^{18}O$ values of CO_2 released from soil collars were derived using the Keeling plot method [51,52] (Figure 1), i.e., from the intercept of the linear regression of $\delta^{13}C$ or $\delta^{18}O$ values of CO_2 against the inverse CO_2 concentration over the closure period ($n = 3$). The coefficients of determination (R^2) for these regressions were generally greater than 0.95 for $\delta^{13}C$-CO_2 and greater than 0.80 for $\delta^{18}O$-CO_2. Soil temperature and volumetric water content (%, v/v) at 7 cm depth within the collars were simultaneously recorded using a temperature-moisture combination probe attached to the portable gas analyzer (915-0011, Los Research Inc., Fremont, CA, USA) (Figure 1) [50]. These auxiliary measurements allowed us to explore the mechanisms underlying the observed variations in $\delta^{13}C$ and $\delta^{18}O$ values of soil-respired CO_2.

2.4. Calculation and Statistical Analysis

Headspace CO_2 and CH_4 concentrations measured by the portable greenhouse gas analyzer (915-0011, Los Research Inc., Fremont, CA, USA) changed linearly over the closure period, and soil collar carbon fluxes were calculated from these changes [50]. Soil CO_2 and CH_4 fluxes were expressed as μmol CO_2 m^{-2} s^{-1} and nmol CH_4 m^{-2} s^{-1}, respectively. To partition CO_2 emitted from C-amended soils (with and without N co-addition), we applied a two-end-member isotopic mixing model [53]. The fraction of CO_2 derived from the added sucrose ($f_{sucrose}$) was calculated as:

$$f_{sucrose} = (\delta^{13}C_{treated} - \delta^{13}C_{non\text{-}treated})/(\delta^{13}C_{sucrose} - \delta^{13}C_{non\text{-}treated}) \quad (2)$$

and the non-substrate-derived CO_2 emission was calculated as:

$$\begin{aligned} F_{non\text{-}substrate} &= F_{total} \times (1 - f_{sucrose}) \\ &= F_{total} \times (\delta^{13}C_{sucrose} - \delta^{13}C_{treated})/(\delta^{13}C_{sucrose} - \delta^{13}C_{non\text{-}treated}) \end{aligned} \quad (3)$$

where $F_{non\text{-}substrate}$ and F_{total} denote the non-substrate-derived CO_2 and total CO_2 emissions (μmol CO_2 m^{-2} s^{-1}) from C-amended soils, respectively; $\delta^{13}C_{treated}$ is the $\delta^{13}C$ value of CO_2 released from C-amended soil (‰); $\delta^{13}C_{non\text{-}treated}$ is that from the control soil without C and N additions (‰); and $\delta^{13}C_{sucrose}$ is the $\delta^{13}C$ value of the added sucrose (−12‰). This calculation assumes that the added sucrose and native soil organic matter are the two dominant respiratory C sources and that any priming effect is operationally included in the non-substrate fraction.

All measured variables were tested for normality using the Shapiro–Wilk test and for homogeneity of variance using Levene's test, and log-transformation was applied where necessary. The $\delta^{13}C$ and $\delta^{18}O$ values of soil-respired CO_2 were analyzed separately for forest and lawn using two-way repeated-measures ANOVA, with treatment and season as fixed effects. A separate two-way repeated-measures ANOVA, with treatment and the number of C and N additions as fixed factors, was used to assess their effects on $\delta^{13}C$ and $\delta^{18}O$ within each season for both vegetation types. A three-way repeated-measures ANOVA, with treatment, vegetation type, and season as fixed effects, were used to evaluate their influences across all three seasons. Pairwise comparisons were conducted using Tukey's HSD *post hoc* tests ($\alpha = 0.05$). Box plots of $\delta^{13}C$ and $\delta^{18}O$ values were generated using OriginPro 2021 (OriginLab Corporation, Northampton, MA, USA). The values were grouped by land cover (forest and lawn) and by treatment for each season ($n = 24$ per group) and across all three seasons ($n = 72$ per group). All statistical analyses were performed with SPSS (version 19.0, IBM Corp., New York, NY, USA).

To explore the combined effects of soil temperature and moisture at 7 cm depth, non-substrate-derived CO_2 emission, and CH_4 flux on the $\delta^{13}C$ and $\delta^{18}O$ values of

soil-respired CO_2, contour analyses were conducted for forest and lawn stands across all treatments and seasons. Multivariate regression curves were fitted using OriginPro 2021. Scatter plots were constructed to illustrate the influences of CH_4 uptake, non-substrate-derived CO_2 emission, soil moisture and temperature at 7 cm depth on $\delta^{13}C$ and $\delta^{18}O$, categorized by treatment, season, and vegetation type. Linear and non-linear regressions were fitted as appropriate using OriginPro 2021. Based on preliminary principal component analyses, soil moisture, soil temperature, non-substrate-derived CO_2 emission, and CH_4 uptake were selected as predictors to construct an a priori structural equation model (SEM) to evaluate the direct and indirect pathways affecting $\delta^{13}C$ and $\delta^{18}O$, using a dataset of 576 paired observations. Model fit was assessed using the comparative fit index (CFI), the chi-squared test, and the root-mean-square error of approximation (RMSEA). The SEM analysis was performed using AMOS 24 (SPSS Inc., Chicago, IL, USA).

3. Results

3.1. Effects of C and N Additions on $\delta^{13}C$ and $\delta^{18}O$ Values of Soil-Respired CO_2

Across the three seasons, sucrose addition alone produced mean $\delta^{13}C$ values of soil-respired CO_2 ranging from –21.33‰ to –19.34‰ under forest and from –20.89‰ to –19.23‰ under lawn, with the lowest values consistently observed in summer (Tukey HSD, $p < 0.001$). These values were significantly higher than those of the control (Tukey HSD, $p < 0.001$), which ranged from –22.61‰ to –20.55‰ under forest and from –22.13‰ to –20.55‰ under lawn (Figure 2a). Notably, no significant differences in $\delta^{13}C$ were detected between the N + C and C-alone treatments (Figure 2a). Nitrogen addition alone tended to increase $\delta^{13}C$, particularly under forest, but this effect did not differ significantly from the control within or across seasons (Figure 2a). Relative to both the control and N-alone treatments, N + C addition resulted in less ^{13}C-depleted soil-respired CO_2 under lawn in autumn, spring, and across the three seasons, and under forest in spring and across the three seasons (Tukey HSD, $p < 0.05$; Figure 2a). In summer, however, no significant treatment effects were detected, except that the C-alone treatment exhibited higher $\delta^{13}C$ of soil-respired CO_2 than the control (Tukey HSD, $p < 0.05$; Figure 2a). A significant treatment × season interaction was detected for $\delta^{13}C$ of soil-respired CO_2 under both forest and lawn ($p < 0.01$; Figure 2a).

For $\delta^{18}O$ values of soil-respired CO_2, C addition alone yielded mean values ranging from –31.16‰ to –22.55‰ under forest and from –31.27‰ to –23.13‰ under lawn, again with summer minima (Tukey HSD, $p < 0.001$ for both; Figure 2b). On average, these values were significantly lower than those of the control across the three seasons, which ranged from –27.92‰ to –19.42‰ under forest and from –28.57‰ to –19.53‰ under lawn (Tukey HSD, $p < 0.01$; Figure 2b). As with $\delta^{13}C$, no significant differences in $\delta^{18}O$ were observed between the N + C and C-alone treatments (Figure 2b). Nitrogen addition alone tended to elevate $\delta^{18}O$, especially under forest, but this effect was not statistically significant relative to the control (Figure 2b). Compared with N addition alone, the N + C treatment caused greater ^{18}O depletion in soil-respired CO_2 under forest in autumn and spring (Tukey HSD, $p < 0.01$) and across all three seasons (Tukey HSD, $p < 0.001$) (Figure 2b). Under lawn, the N + C treatment likewise resulted in greater ^{18}O depletion across the three seasons than N alone (Tukey HSD, $p < 0.05$; Figure 2b). No significant treatment × season interaction was observed for $\delta^{18}O$ of soil-respired CO_2 under either forest or lawn (Figure 2b).

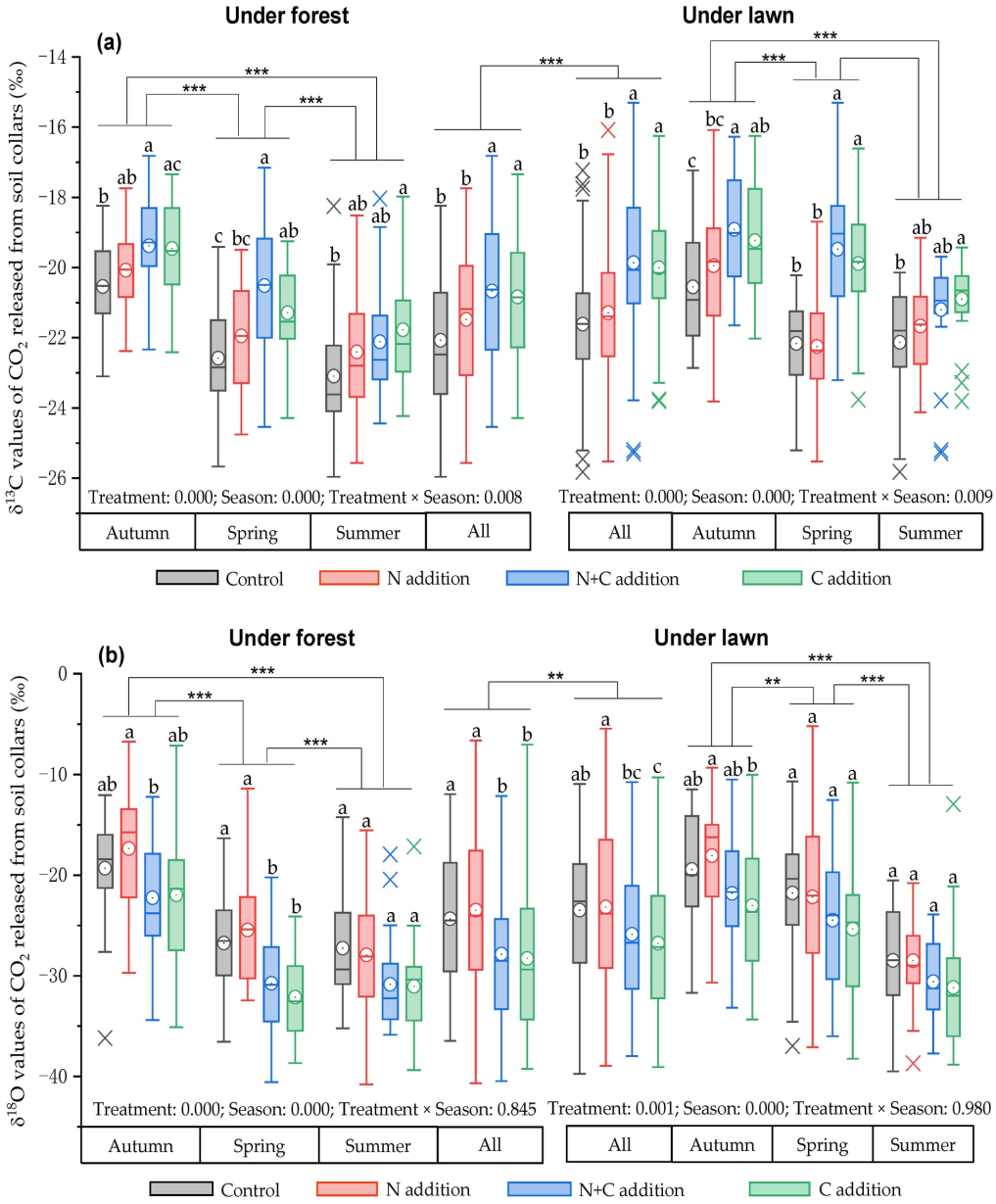

Figure 2. Box plots of $\delta^{13}C$ (**a**) and $\delta^{18}O$ (**b**) values of CO_2 released from soil collars under forest and lawn in each season and across all three seasons during the two carbon and nitrogen addition experiments. Boxes represent interquartile ranges (IQRs), with circles and horizontal lines inside the boxes indicating mean and median values, respectively. The lower and upper whiskers extend to the 25th percentiles minus 1.5 × IQR and the 75th percentiles plus 1.5 × IQR, respectively. Diagonal crosses indicate outliers. Boxes labelled with different lowercase letters indicate significant differences (Tukey's HSD *post hoc* test, $p < 0.05$) in mean $\delta^{13}C$ and $\delta^{18}O$ of soil-respired CO_2 between treatments under forest and lawn, either within each season or across all three seasons. "All" refers to all three seasons combined. ANOVA results (p values) for treatment and season as fixed factors for forest and lawn are shown. Significant differences in mean $\delta^{13}C$ and $\delta^{18}O$ values among seasons under forest and lawn, and between vegetation types, are indicated by ** ($p < 0.01$) and *** ($p < 0.001$).

3.2. Effects of Vegetation Type and Season on $\delta^{13}C$ and $\delta^{18}O$ Values of Soil-Respired CO_2

Regardless of C and N addition, soil-respired CO_2 under forest exhibited significantly lower mean $\delta^{13}C$ and $\delta^{18}O$ values (–21.26 ± 0.11‰ and –26.09 ± 0.42‰, respectively) than under lawn (–20.69 ± 0.11‰ and –24.67 ± 0.43‰, respectively) (Tukey HSD, $p < 0.01$ for both; Figure 2a,b). Across all four treatments, both vegetation types showed pronounced

seasonal variation in the isotopic composition of soil-respired CO_2 (Tukey HSD, $p < 0.01$). Specifically, $\delta^{13}C$ peaked in autumn (–19.76 ± 0.12‰) and reached a minimum in summer (–21.91 ± 0.12‰), whereas $\delta^{18}O$ values were highest in autumn (–20.45 ± 0.45‰) and lowest in summer (–29.53 ± 0.39‰) (Figure 2a,b).

3.3. Relationships Between the Isotopic Composition of Soil-Respired CO_2, Soil CH_4 Flux, and Non-Substrate-Derived CO_2 Emission

Across all four treatments, $\delta^{13}C$ values of soil-respired CO_2 increased significantly and non-linearly with rising non-substrate-derived CO_2 emission under both forest and lawn ($p < 0.001$; Figure 3a). In parallel, $\delta^{18}O$ values of soil-respired CO_2 decreased significantly and non-linearly as non-substrate-derived CO_2 emission increased across all treatments and seasons ($p < 0.001$; Figure 3b). When treatments and vegetation types were analyzed separately, $\delta^{18}O$-CO_2 values within each treatment and in either vegetation type consistently decreased in a significant, non-linear manner with both greater soil CH_4 uptake ($p < 0.05$; Figures 4a–d and 5a,b) and enhanced non-substrate-derived CO_2 emission ($p < 0.001$; Figures 4e–h and 5c,d). Notably, the model fit improved from forest to lawn (Figure 5), with the best fit observed in the N-alone treatment among all four treatments (Figure 4).

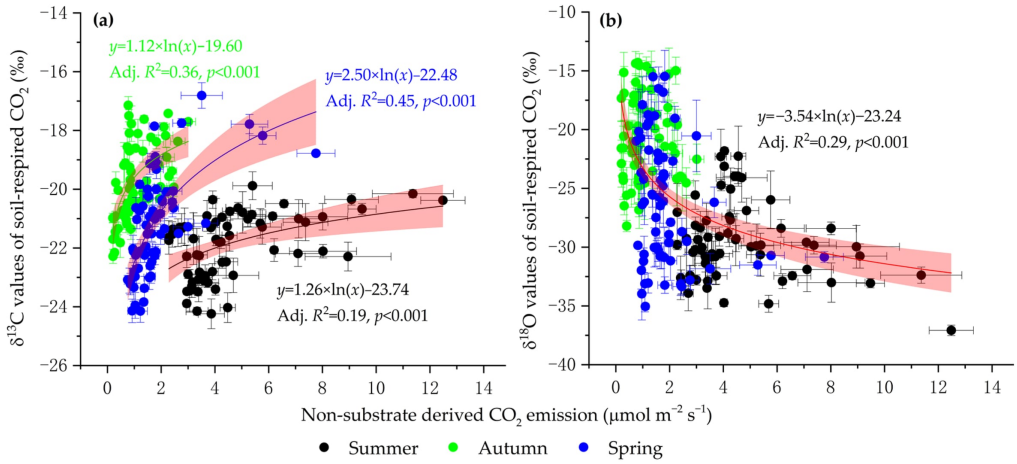

Figure 3. Relationships between non-substrate-derived CO_2 emission from soil collars (x) and the $\delta^{13}C$ (**a**) and $\delta^{18}O$ (**b**) values of soil-respired CO_2 (y) across all treatments and seasons under forest and lawn. Non-linear regressions were used to examine these relationships, with separate regressions fitted for $\delta^{13}C$ in each season and a single regression fitted for $\delta^{18}O$ using data pooled across all three seasons. Shaded areas indicate the 95% confidence bands of the non-linear regressions.

In contrast to $\delta^{18}O$-CO_2, a significant negative relationship between $\delta^{13}C$-CO_2 values and non-substrate-derived CO_2 emissions was detected only in the control of both vegetation types ($p < 0.05$; Figures S1e–h and S2c,d). However, similar to the pattern observed for $\delta^{18}O$-CO_2, $\delta^{13}C$-CO_2 values decreased significantly with increasing soil CH_4 uptake in both vegetation types and in the control and N-alone treatments ($p < 0.05$), with relatively stronger model fits under lawn and in the control (Figures S1a,b and S2a,b). Collectively, non-substrate-derived CO_2 emission and soil CH_4 uptake accounted for 12% and 27% of the observed variation in $\delta^{13}C$ and $\delta^{18}O$ of soil-respired CO_2, respectively, under the experimental conditions ($p < 0.001$; Figure 6c,d).

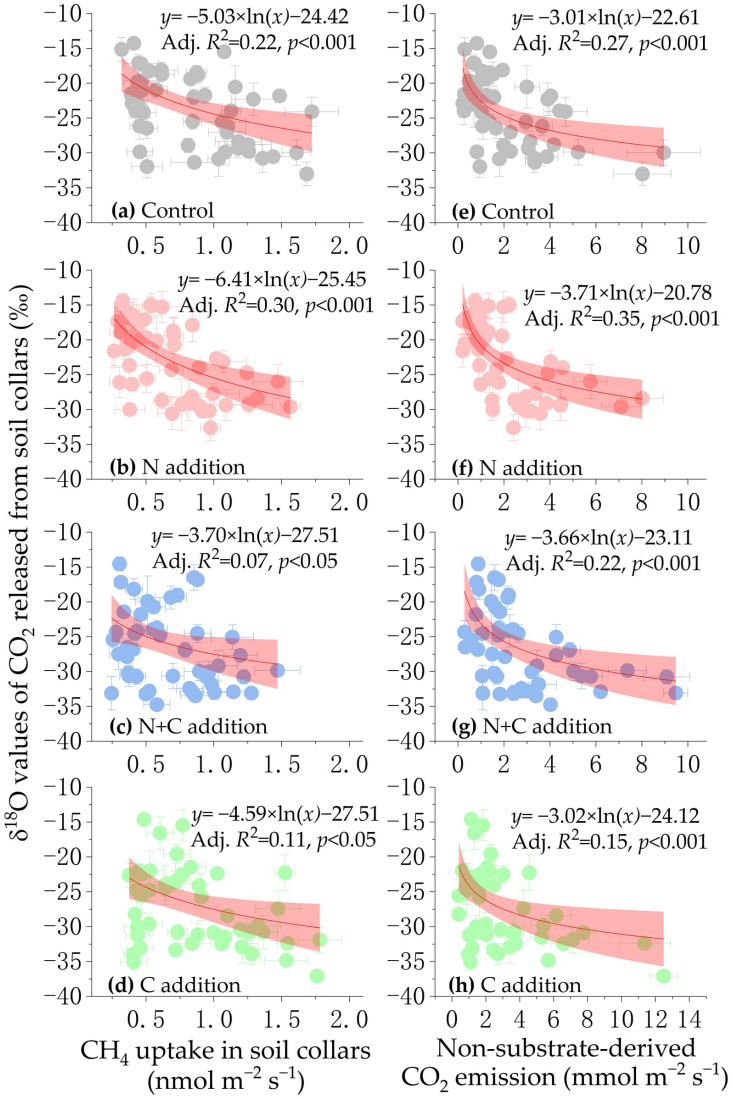

Figure 4. Relationships between $\delta^{18}O$ values of soil-respired CO_2 (y) and soil CH_4 uptake (**a**–**d**) or non-substrate-derived CO_2 emission (**e**–**h**) (x) in each treatment across all three seasons under forest and lawn. Shaded areas indicate the 95% confidence bands of the non-linear regressions.

3.4. Relationships Between the Isotopic Composition of Soil-Respired CO_2, Temperature, and Moisture

Under the experimental conditions, soil moisture and temperature at 7 cm depth jointly explained 22% and 27% of the variation in $\delta^{13}C$ and $\delta^{18}O$ of soil-respired CO_2, respectively ($p < 0.001$; Figure 6a,b). When examined separately, both isotopic signatures increased significantly and linearly with rising soil moisture across the range of 10–50% (v/v) ($p < 0.001$), with the model fit improving from forest to lawn (Figure 7a,b). In contrast, both $\delta^{13}C$ and $\delta^{18}O$ declined significantly and linearly with increasing soil temperature over the range from near zero to 30 °C ($p < 0.001$), with notably stronger model fits for $\delta^{18}O$ under both forest and lawn (Figure 7c,d).

To further explore the underlying drivers, we performed a structural equation modelling (SEM) analysis using the paired observation dataset ($n = 576$), which included soil CH_4 flux, non-substrate-derived CO_2 emission, and soil moisture and temperature. These variables collectively accounted for 18% and 20% of the variation in $\delta^{13}C$ and $\delta^{18}O$ under both forest and lawn, respectively (Figure 8a). Soil moisture and temperature exerted similar directional effects on both isotopes, yet soil moisture had a relatively stronger influence on $\delta^{13}C$ (Figure 8b), whereas soil temperature played a more prominent role in shaping

$\delta^{18}O$ (Figure 8c). Within the SEM framework, soil CH_4 flux and non-substrate-derived CO_2 emission showed opposing effects on $\delta^{13}C$ and $\delta^{18}O$, respectively (Figure 8b,c).

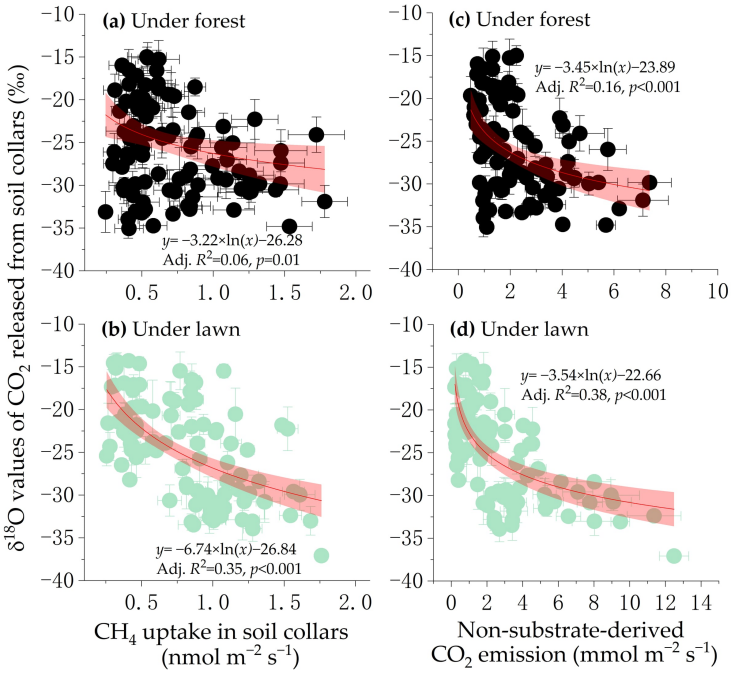

Figure 5. Relationships between $\delta^{18}O$ values of soil-respired CO_2 (y) and soil CH_4 uptake (**a**,**b**) or non-substrate-derived CO_2 emission (**c**,**d**) (x) under forest and lawn across all three seasons. Shaded areas indicate the 95% confidence bands of the non-linear regressions.

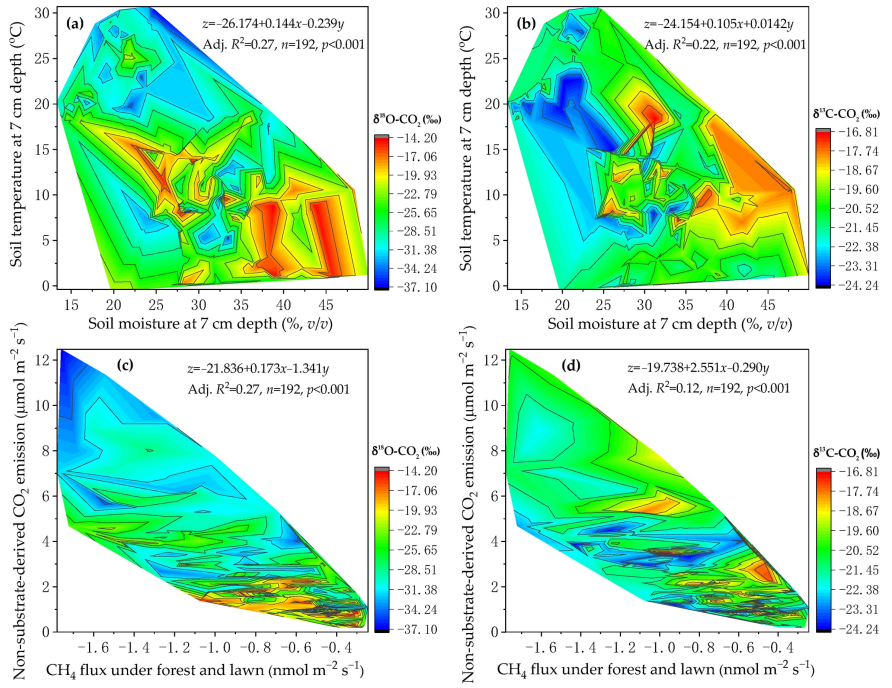

Figure 6. Combined effects of soil temperature and moisture at 7 cm depth (**a**,**b**) and of non-substrate-derived CO_2 emission and CH_4 flux (**c**,**d**) on the $\delta^{13}C$ and $\delta^{18}O$ values of soil-respired CO_2 under forest and lawn across all treatments and seasons. Multivariate regression surfaces were fitted with soil moisture (x) and soil temperature (y), or CH_4 flux (x) and non-substrate-derived CO_2 emission (y), as predictors of $\delta^{13}C$ and $\delta^{18}O$ (z); x, y, and z are means of three replicates per measurement. Legend colors represent different ranges of $\delta^{13}C$ and $\delta^{18}O$ values.

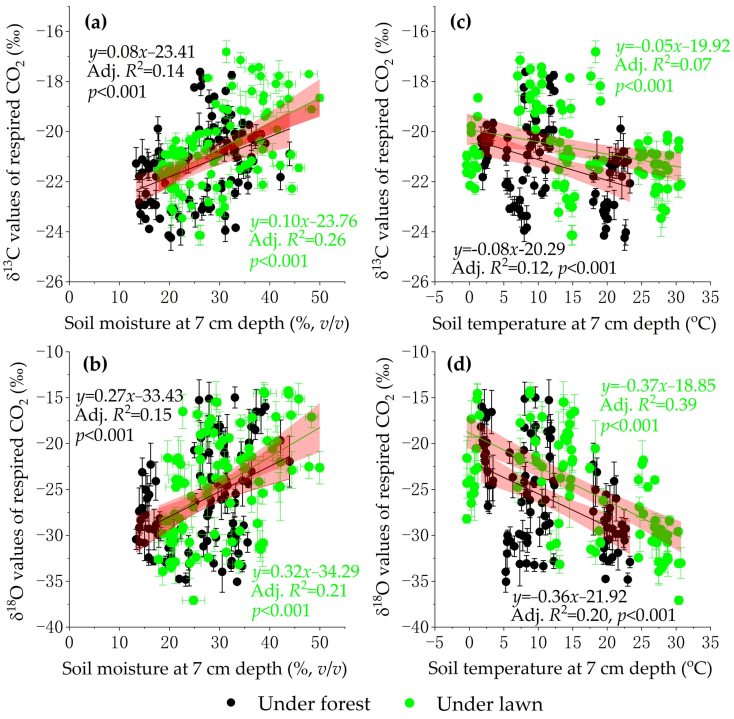

Figure 7. Relationships of $\delta^{13}C$ and $\delta^{18}O$ values of soil-respired CO_2 (y) and soil moisture (**a**,**b**) or temperature (**c**,**d**) (x) at 7 cm depth across all seasons under forest and lawn. Shaded areas indicate the 95% confidence bands of the linear regressions (black for forest, green for lawn).

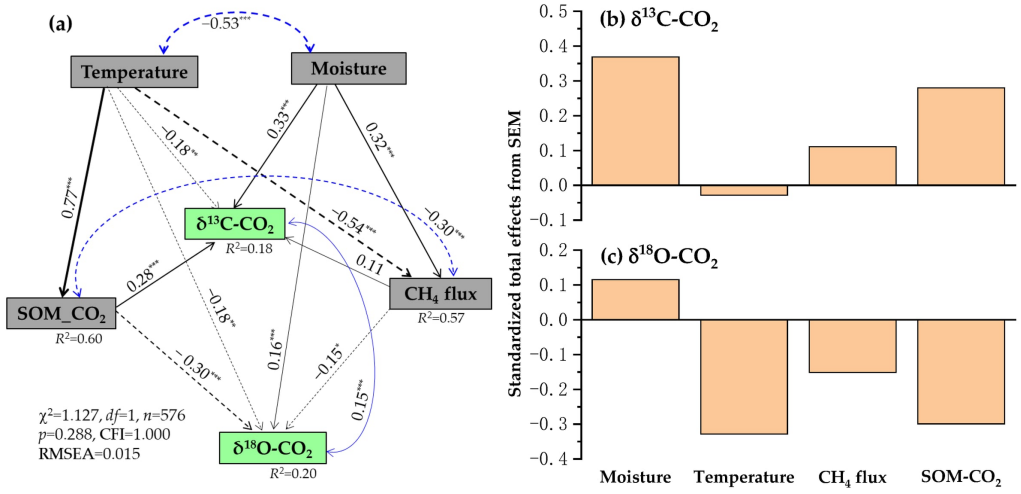

Figure 8. Structural equation modeling (SEM) analysis of causal relationships among temperature, moisture, CH_4 flux, SOM_CO_2, $\delta^{13}C$-CO_2, and $\delta^{18}O$-CO_2 under forest and lawn across all treatments and seasons (**a**), and their standardized total effects on $\delta^{13}C$-CO_2 (**b**) and $\delta^{18}O$-CO_2 (**c**). Temperature and moisture denote soil temperature and moisture at 7 cm depth, respectively; SOM_CO_2 denotes non-substrate derived CO_2 emission; and $\delta^{13}C$-CO_2 and $\delta^{18}O$-CO_2 denote the $\delta^{13}C$ and $\delta^{18}O$ values of soil-respired CO_2, respectively. Single-headed arrows indicate the hypothesized direction of causation, whereas double-headed arrows represent correlations between covariances of variables. The width of arrows is proportional to the strength of the relationship. Numbers adjacent to arrows are standardized regression or correlation coefficients, and R^2 values represent the proportion of variation explained by relationships with other variables. χ^2, RMSEA, and CFI denote the Chi-square, root-mean-square error of approximation, and comparative fit index, respectively. n, p, and df represent the number of paired observations, the probability level, and the degrees of freedom, respectively. *, $p < 0.05$; **, $p < 0.01$; ***, $p < 0.001$.

4. Discussion

4.1. Divergent Regulation of the Isotopic Signature of Soil Respiration by C and N Additions

Carbon addition as sucrose significantly altered both $\delta^{13}C$ and $\delta^{18}O$ of soil-respired CO_2 under forest and lawn, but in opposite directions: C addition alone enriched $\delta^{13}C$ while depleting $\delta^{18}O$ relative to the control (Figure 2a,b). This contrast is the central prediction of H1, namely that the two isotopes respond to distinct regulatory mechanisms and therefore carry different isotopic imprints of soil respiration [54,55]. It also frames H3, since the direction of each response differs between the single additions.

The $\delta^{13}C$ enrichment can arise directly from mixing with the added sucrose, which has a $\delta^{13}C$ value of −12‰ and is therefore ^{13}C-enriched relative to native soil organic matter. Fresh organic C may additionally stimulate microbial decomposition of native soil organic matter, and shifts in substrate availability may alter microbial C-use patterns [7,56,57]. Because the carbon isotopic composition of soil-respired CO_2 is closely tied to that of the respiratory substrate pool, any factor that changes substrate availability can systematically affect $\delta^{13}C$–CO_2 [30,55,56]. Our design cannot separate direct substrate mixing from priming or from preferential microbial use of specific substrates; hence, the observed $\delta^{13}C$ enrichment should not be attributed solely to a priming effect.

The marked $\delta^{18}O$ depletion induced by C addition is mechanistically less direct and is consistent with the gas-transport control posited in H1. It may arise from altered CO_2–H_2O oxygen exchange, whose equilibrium fractionation depends strongly on temperature and moisture [22,30,58]. Carbon addition may change CO_2 residence time and diffusion pathways by modifying microbial activity [20,22,58], thereby shifting the degree of oxygen isotopic exchange between CO_2 and soil water. This interpretation is consistent with the high sensitivity of $\delta^{18}O$ to non-substrate-derived CO_2 emission and soil CH_4 uptake observed here (Figures 4 and 5). Specifically, C addition could lower $\delta^{18}O$ by (1) accelerating CO_2 production and shortening CO_2 residence time in soil pores, thus weakening oxygen exchange equilibrium with soil water, which is less ^{18}O-depleted than dissolved CO_2 [59], and (2) altering soil pore structure or water distribution and thus CO_2 diffusion and transport efficiency. Because the $\delta^{18}O$ of soil-respired CO_2 is highly sensitive to gas exchange and transport in soil [58], the opposite responses of $\delta^{13}C$ and $\delta^{18}O$ to C addition reflect their differing controls: $\delta^{13}C$ is predominantly substrate-driven, whereas $\delta^{18}O$ is more strongly influenced by gas transport and exchange. Because soil-water $\delta^{18}O$ was not measured, these mechanisms remain inferred rather than directly demonstrated.

Nitrogen addition alone had no statistically significant effect on either $\delta^{13}C$ or $\delta^{18}O$, except for a slight enrichment trend under forest, which is consistent with the weak N effect predicted in H1. This result may be attributable to several factors: (1) the studied ecosystems may be primarily C-limited rather than N-limited, resulting in a weak microbial response to N addition; (2) N addition may simultaneously stimulate microbial utilization of both ^{13}C-enriched and ^{13}C-depleted substrates, with their effects counterbalancing each other [26,29,60]; and (3) N-induced changes in soil pH or microbial community composition during a relatively short-term period may not have reached the threshold required to alter the respiratory isotopic signal [28,61]. These remain candidate explanations because soil pH and microbial community composition were not measured. The N + C treatment generally produced higher seasonal mean $\delta^{13}C$ and lower $\delta^{18}O$ than N addition alone ($p < 0.05$), but did not differ significantly from C addition alone. This pattern addresses H3: it suggests that C availability can modulate N-induced isotopic fractionation, or, more conservatively, that the isotopic effect of the combined treatment is dominated by C addition rather than by an independent N effect; hence, the interaction is closer to additive-with-C-dominance than to a strong non-additive C × N effect. This interpretation implies that, under increasing

atmospheric N deposition, the isotopic response of soil respiration to exogenous N input may depend critically on soil C availability [30,62–64].

4.2. Vegetation Type and Season Dominate the Spatiotemporal Patterns of the Isotopic Composition of Soil-Respired CO_2

Vegetation type significantly shaped the isotopic composition of soil-respired CO_2 (Figure 2a,b), as predicted by H2. Across all treatments and seasons, mean $\delta^{13}C$ and $\delta^{18}O$ of soil-respired CO_2 under forest were –21.26‰ and –26.09‰, respectively, both significantly lower than those under lawn (–20.69‰ and –24.67‰; $p < 0.05$). These values fall within the ranges previously reported for temperate forests and grasslands [12,21,59,65,66]. Several non-exclusive explanations are plausible. First, forest soil organic matter is generally more ^{13}C-depleted than grassland soil organic matter, reflecting the dominance of C3 vegetation under forest versus possible presence of C4 species under lawn. Greater root respiration under forest may further lower the $\delta^{13}C$ of forest soil respiration, because root-derived CO_2 is typically ^{13}C-depleted relative to $\delta^{13}C$ values in aboveground tissues [12,18,38]. Second, forest soils often have thicker litter layers and older, more ^{13}C-depleted organic matter, and decomposition of different organic matter fractions can shape the isotopic composition of released CO_2 [67]. Third, the $\delta^{18}O$ difference likely reflects contrasting hydrology and plant physiology. In forests, precipitation is a dominant water source with lower $\delta^{18}O$ than leaf water, whereas transpiration can enrich lawn leaf water in ^{18}O, potentially leading to higher $\delta^{18}O$ in the CO_2 released from lawn soil. In addition, moss cover on forest floors may further modify soil microclimate and has been linked to lower $\delta^{13}C$ of soil-respired CO_2 [30]. The forest–lawn isotopic contrast therefore appears to emerge from a cascade of processes spanning photosynthetic carbon assimilation, root respiration, organic matter turnover, soil hydrology, and gas exchange, rather than from a single dominant factor.

Seasonally, the mean $\delta^{13}C$ and $\delta^{18}O$ values of soil-respired CO_2 across all treatments under forest and lawn reached their respective minima in summer and maxima in autumn (Tukey HSD, $p \leq 0.001$; Figure 2a,b). The lowest $\delta^{13}C$ values in summer may reflect enhanced root and rhizosphere respiration of fresh, recently assimilated photosynthates, which typically carry more negative $\delta^{13}C$ signatures under high air humidity [18,40,68]. Because total soil respiration integrates autotrophic and heterotrophic sources, this signal may be further modified by temperature-driven shifts in microbial substrate use and by CO_2 diffusion fractionation under non-steady-state transport [66,69]. In a northern Japanese deciduous needle-leaf forest, heterotrophic respiration $\delta^{13}C$ was lower in warm than in cool seasons [66]. Werner et al. [55] similarly emphasized that the mixing of recent photosynthates with stored C reserves drives seasonal $\delta^{13}C$ dynamics. The summer $\delta^{18}O$ minimum may be linked to evaporative changes in soil-water $\delta^{18}O$, high non-substrate-derived CO_2 emission (Figure S3b), and altered CO_2–H_2O oxygen exchange [22]. Previous studies have shown that the $\delta^{18}O$ of soil-respired CO_2 exhibits a significant nonlinear relationship with soil temperature and moisture [20,30,59], with warmer conditions intensifying diffusion and exchange rates and lowering $\delta^{18}O$. Collectively, seasonal environmental shifts influence forest and lawn soil-respired CO_2 $\delta^{13}C$ and $\delta^{18}O$ through distinct pathways, supporting dual-isotope analysis as a means to comprehensively explore carbon–water relationships in the soil–plant continuum across temporospatial scales [55,70]. Consistent with H2, both vegetation type and season imposed stronger contrasts in soil-respired CO_2 $\delta^{13}C$ and $\delta^{18}O$ values than the nutrient treatments themselves.

4.3. Contrasting Controls of Soil Temperature and Moisture on the Isotopic Signatures of Soil Respiration

Contour analysis showed that soil moisture and temperature jointly explained 22% and 27% of the variance in $\delta^{13}C$ and $\delta^{18}O$, respectively (Figure 6a,b). Moisture exerted a stronger standardized total effect on $\delta^{13}C$, whereas temperature exerted a stronger standardized total effect on $\delta^{18}O$ (Figure 8b,c). These standardized effects should not be read as evidence that moisture is the sole control of $\delta^{13}C$ or that temperature is the sole control of $\delta^{18}O$. The two predictors were correlated, and the SEM explained only 18% and 20% of the variance in $\delta^{13}C$ and $\delta^{18}O$, respectively (Figure 8a), leaving substantial variation attributable to unmeasured substrate, microbial, and soil-water properties. The contrasting effects are therefore better interpreted within a mechanistic framework of H1: $\delta^{13}C$ is primarily propagated from the respiratory substrate pool, whereas $\delta^{18}O$ is strongly influenced by CO_2–H_2O oxygen exchange and gas transport [22,30,55,59].

The stronger control of moisture on $\delta^{13}C$ is consistent with the substrate-centered nature of carbon isotope fractionation. The soils in this study are sandy-textured and remain persistently below field moisture capacity. Under such conditions, moisture regulates the diffusion of soluble organic C and extracellular enzymes, the accessibility of organic matter to microbes, O_2 availability, microbial carbon-use efficiency, and the relative contributions of root and microbial respiration [7,30,55,57]. Increased soil moisture can alleviate substrate diffusion limitation and enhance microbial access to soil organic matter, potentially shifting respiration toward older, ^{13}C-enriched organic matter or altering the balance among respiratory substrate pools. Because diffusive fractionation of CO_2 has only a minor effect on $\delta^{13}C$ relative to the large isotopic differences among photosynthetic inputs, soil organic matter fractions, and microbial substrates, changes in substrate supply and microbial substrate use can be recorded as systematic shifts in $\delta^{13}C$–CO_2 [30,55]. Soil moisture may also modify the balance between root and microbial contributions, which differ in their isotopic end-members, thereby further affecting the bulk $\delta^{13}C$ signal [18,38]. Furthermore, high soil CH_4 uptake under low moisture [71] would contribute to the lower $\delta^{13}C$ of CO_2 accumulated in the soil collars after closure, because biogenic CH_4 has an average $\delta^{13}C$ of approximately –63.0‰ [47]. Taken together, these mechanisms provide a biophysical basis for the positive $\delta^{13}C$–moisture relationship observed across the 10–50% (v/v) range (Figure 7a,b), although the present design cannot separate direct substrate mixing from priming or from microbial substrate preference.

The stronger control of temperature on $\delta^{18}O$ is mechanistically expected, because oxygen isotope exchange between CO_2 and soil water is controlled by both thermodynamics and kinetics. The equilibrium fractionation between CO_2 and H_2O depends on temperature, and the rate at which respiratory CO_2 approaches isotopic equilibrium with soil water is accelerated by carbonic anhydrase and by higher temperatures [22,30,58,59]. Temperature therefore influences both the equilibrium end-member and the degree to which respiratory CO_2 retains a kinetic or diffusive signature before diffusing out of the soil. Temperature also affects CO_2 diffusion, soil evaporation, and the $\delta^{18}O$ of soil water, all of which can propagate into $\delta^{18}O$–CO_2 [20,34,72]. The observed negative $\delta^{18}O$–temperature relationship over the near 0–30 °C range (Figure 7c,d) is consistent with a shift toward less ^{18}O-enriched CO_2 relative to soil water as temperature rises, although soil-water $\delta^{18}O$ was not measured and therefore cannot be used to close the isotope mass balance. The positive $\delta^{18}O$–moisture relationship across 10–50% (v/v) (Figure 7a,b) is likewise consistent with greater CO_2–H_2O exchange and altered gas transport under wetter conditions, but it may also reflect moisture effects on soil-water $\delta^{18}O$ and on the degree of exchange equilibrium.

Temperature also influences $\delta^{13}C$ through microbial metabolism, substrate preference, and diffusion, whereas moisture affects $\delta^{18}O$ through exchange and transport. The SEM

contrasts therefore indicate relative rather than exclusive control, which is itself the H2 prediction: season (the temperature–moisture regime) modulates treatment effects more strongly than vegetation type. Consistent with this, $\delta^{13}C$ and $\delta^{18}O$ responded in opposite directions to soil moisture and temperature, while non-substrate-derived CO_2 emission increased exponentially with temperature (Figure S3b) and peaked at intermediate moisture (approximately 20–25%, *v*/*v*) (Figure S3a) [73]. These patterns suggest that temperature and moisture jointly modulate CO_2 production and the isotopic composition of the emitted CO_2 through distinct but coupled pathways. The opposing SEM effects of CH_4 flux and non-substrate-derived CO_2 emission on $\delta^{13}C$ and $\delta^{18}O$ (Figure 8b,c) should be interpreted cautiously, because these fluxes are correlational indicators of soil pore structure, gas transport, and substrate dynamics rather than direct isotopic controls. In particular, because non-substrate-derived CO_2 was calculated from $\delta^{13}C$ using Equations (2) and (3), its inclusion as a predictor of $\delta^{13}C$ introduces part–whole coupling, and the corresponding SEM path should therefore be regarded as an accounting relationship rather than an independent causal pathway.

Overall, the SEM results are best understood as statistical summaries of a mechanistic hierarchy consistent with H1: moisture is a proximal control of substrate accessibility and microbial substrate use, which are the dominant determinants of $\delta^{13}C$–CO_2, whereas temperature is a proximal control of CO_2–H_2O exchange thermodynamics and kinetics, which are the dominant determinants of $\delta^{18}O$–CO_2. This hierarchy explains why $\delta^{18}O$ responded more strongly than $\delta^{13}C$ to temperature (Figure 7c,d) and why moisture exerted a stronger total effect on $\delta^{13}C$ than on $\delta^{18}O$ (Figure 8b,c). Because soil-water $\delta^{18}O$, carbonic anhydrase activity, microbial community composition, and substrate isotopic end-members were not measured, these mechanistic interpretations remain hypotheses. Future work should combine concurrent soil-water $\delta^{18}O$ monitoring, microbial and enzyme measurements, characterization of substrate isotopic end-members, separation of root and microbial respiration, and factorial moisture–temperature manipulation to test the proposed pathways directly.

4.4. High Sensitivity of $\delta^{18}O$ of Soil-Respired CO_2 to Abiotic Processes and Its Indicative Significance

A key finding of this study is the strong nonlinear negative correlation of $\delta^{18}O$ in soil-respired CO_2 with both soil CH_4 uptake and non-substrate-derived CO_2 emission ($p < 0.001$; Figure 5b,d). Together, the two carbon fluxes explained 27% of the variance in $\delta^{18}O$ ($p < 0.001$; Figure 6c). In contrast, $\delta^{13}C$ was much more weakly related to the same variables, reaching significance only in the control ($p < 0.05$; Figure S1a,e) and explaining only 12% of the variance (Figure 6d). The SEM further indicated that the two carbon fluxes had contrasting effects on $\delta^{18}O$ and $\delta^{13}C$ (Figure 8b,c). This disparity directly expresses H1: the two isotopes track distinct ecological processes and provide different perspectives on soil carbon dynamics. These relationships are correlational and do not establish that CH_4 oxidation or non-substrate CO_2 emission directly controls $\delta^{18}O$.

The high sensitivity of $\delta^{18}O$-CO_2 to gas transport arises from oxygen isotope fractionation during diffusion: the lighter isotopologue ($C^{16}O^{16}O$) diffuses slightly faster than the heavier one ($C^{18}O^{16}O$). Enhanced CH_4 uptake or increased non-substrate-derived CO_2 emission may therefore reflect changes in soil pore structure and diffusion conditions, which in turn could systematically alter the oxygen isotopic composition of soil CO_2. Beyond diffusion, the $\delta^{18}O$ of soil-respired CO_2 is strongly modulated by oxygen exchange between CO_2 and soil water. Processes that alter soil moisture or gas residence time, such as CH_4 oxidation and biotic CO_2 emissions, can shift the CO_2–H_2O exchange equilibrium and thus $\delta^{18}O$. The negative $\delta^{18}O$–CH_4 uptake correlation observed here suggests that CH_4 oxidation may modify gas composition and diffusion gradients in soil pores, indirectly affecting

$\delta^{18}O$-CO_2. Such indirect effects warrant further study, as they imply that $\delta^{18}O$ integrates multiple concurrent physical and biological processes [22,30,34,59,72].

The much weaker relationships between $\delta^{13}C$ of soil-respired CO_2 and the two carbon flux variables support the prevailing view that $\delta^{13}C$ primarily reflects carbon source processes, specifically the isotopic signature of organic matter decomposition, rather than transport or physical exchange [55]. Although soil CO_2 diffusion causes fractionation, its effect on $\delta^{13}C$ is minor relative to the large fractionations during photosynthetic carbon fixation and microbial decomposition. Consistent with this, the relatively small slopes of the linear regressions of $\delta^{13}C$-CO_2 against soil moisture and temperature (Figure 7) indicated that $\delta^{18}O$-CO_2, rather than $\delta^{13}C$-CO_2, becomes more responsive to soil hydrothermal conditions. Thus, $\delta^{13}C$ is better suited to tracing carbon sources and microbial metabolic pathways, whereas $\delta^{18}O$ is more responsive to soil biophysical conditions such as temperature, moisture, and gas diffusion. This functional divergence is the practical value of the H1 framework: using both isotopes together provides a more complete picture of CO_2 production, transport, and exchange in soil.

4.5. Limitations and Future Perspectives

Although this study provides valuable empirical insights into how carbon and nitrogen additions affect the isotopic composition of soil-respired CO_2, several limitations should be considered when interpreting the results. First, soil-water $\delta^{18}O$ was not measured concurrently. Because CO_2–soil water oxygen exchange strongly governs the $\delta^{18}O$ of soil-respired CO_2 [20,22,74], the absence of these data prevents quantitative apportionment of exchange versus respiratory contributions to the observed isotopic signatures. Second, our experimental setup did not separate root-derived (autotrophic) from microbial (heterotrophic) respiration. These pathways differ in substrate sources and isotopic end-members, and their relative contributions can vary seasonally and with shifting environmental condition [4,38], potentially modulating the overall isotopic composition of soil respiration following C and N addition. Third, the relatively short duration of this study limits inference about longer-term trajectories, because priming intensity or even direction may change over time and our dataset cannot capture such temporal dynamics. Fourth, soil pH and microbial community composition were not measured, although both may mediate N effects on substrate use and isotopic fractionation. Finally, the non-substrate-derived CO_2 calculation assumes a two-end-member mixing model and does not explicitly separate priming from native soil organic matter decomposition; this operational definition should be considered when comparing our results with those of other studies.

Future work could address these gaps in several ways. (1) Combined ^{13}C–^{18}O dual labeling would help partition CO_2 sources within total soil respiration. (2) Concurrent monitoring of soil-water $\delta^{18}O$ and soil-air CO_2 $\delta^{18}O$ would permit a more complete oxygen isotope mass balance and a quantitative separation of exchange and respiratory fluxes. (3) Process-based fractionation models, such as ISOLSM [21,75,76], could disentangle diffusion, isotopic exchange, and respiratory production, and may be adapted to assess C and N effects on $\delta^{13}C$ and $\delta^{18}O$ of soil and ecosystem respiration at the canopy scale. (4) Long-term field observations are needed to reveal cumulative effects and interannual variability of C and N additions on the isotopic composition of soil respiration, and to test whether the patterns observed here persist or shift over time [55]. Addressing these gaps would strengthen the mechanistic basis of our findings and improve predictions of soil carbon dynamics under changing environmental conditions.

5. Conclusions and Implications

This study demonstrates that exogenous carbon addition, applied as sucrose, exerts significant yet opposing effects on the $\delta^{13}C$ and $\delta^{18}O$ of soil-respired CO_2: carbon addition enriches $\delta^{13}C$ while depleting $\delta^{18}O$, whereas nitrogen addition has comparatively weak effects. Vegetation type and seasonal variation emerge as important spatiotemporal controls on the isotopic composition of soil respiration. Moreover, $\delta^{18}O$ was more sensitive than $\delta^{13}C$ to environmental factors such as soil CH_4 uptake, non-substrate-derived CO_2 emissions, and soil temperature. These findings indicate that $\delta^{13}C$ and $\delta^{18}O$ play complementary roles in reflecting soil carbon dynamics: $\delta^{13}C$ is more suited to tracing carbon sources and microbial decomposition processes, whereas $\delta^{18}O$ responds more strongly to soil biophysical conditions and gas transport dynamics. The combined use of both isotopic indices therefore supports a more comprehensive understanding of the ecological processes underlying soil respiration. Collectively, this study provides critical process parameters and isotopic constraints for soil carbon cycle models, with theoretical and practical implications for accurately assessing terrestrial carbon budgets. However, quantitative attribution requires concurrent soil-water $\delta^{18}O$ measurements and separation of root and microbial respiration, particularly in comparative studies across different climatic regions and under both short- and long-term C and N inputs.

Supplementary Materials: The following supporting information can be downloaded at: https://www.mdpi.com/article/10.3390/plants15233737/s1, Figure S1. Relationships between $\delta^{13}C$ values of soil-respired CO_2 (y) and CH_4 uptake (**a**–**d**) or non-substrate-derived CO_2 emission (**e**–**h**) (x) for each treatment across all three seasons under forest and lawn. Shaded areas indicate the 95% confidence bands of the non-linear regressions. Figure S2. Relationships between $\delta^{13}C$ values of soil-respired CO_2 (y) and CH_4 uptake (**a**,**b**) or non-substrate-derived CO_2 emission (**c**,**d**) (x) under forest and lawn across all three seasons. Shaded areas indicate the 95% confidence bands of the non-linear regressions. Figure S3. Relationships between non-substrate-derived CO_2 emission (y) and soil moisture (**a**) or temperature (**b**) (x) at 7 cm depth cross all three seasons under forest and lawn. Shaded areas indicate the 95% confidence bands of the non-linear regressions (black for forest, green for lawn).

Author Contributions: Conceptualization, methodology, software, validation, resources, writing—original draft preparation, X.X.; investigation, X.X., J.Y. and W.C.; formal analysis, X.X., W.C., and Y.K.; writing—reviewing and editing, X.X., Y.K., J.Y., W.C., D.K., V.S., and I.K.; data curation, X.X. and Y.K.; projection administration; X.X.; funding acquisition; X.X. and I.K. All authors have read and agreed to the published version of the manuscript.

Funding: This work was supported by the National Natural Science Foundation of China (Grant nos. 42275130 and 42675154), the Beijing Municipal Natural Science Foundation (no. 8262033), and the State assignment of the Ministry of Education and Science of Russia for the Federal Research Center of Biological Research of RAS (#126031118706-8).

Data Availability Statement: The original contributions presented in this study are included in the article/Supplementary Material. Further inquiries can be directed to the corresponding author.

Acknowledgments: The authors thank the National Research Station of Changbai Mountain Forest Ecosystems for support.

Conflicts of Interest: The authors declare no conflicts of interest.

References

1. Bond-Lamberty, B.; Thomson, A. Temperature-associated increases in the global soil respiration record. *Nature* **2010**, *464*, 579–582. [CrossRef] [PubMed]
2. Chen, C.; Chen, H.Y.H. Mapping global nitrogen deposition impacts on soil respiration. *Sci. Total Environ.* **2023**, *871*, 161986. [CrossRef] [PubMed]

3. Zhou, J.J.; Chen, Z.F.; Jian, C.X.; Luo, Y.; Niu, F.R.; Palta, J.A.; Xu, B.C. Autotrophic respiration is more sensitive to nitrogen and phosphorus supply than heterotrophic respiration in semiarid grassland. *J. Geophys. Res.-Biogeo.* **2024**, *129*, e2024JG008230. [CrossRef]
4. Lv, W.W.; Li, J.W.; Dong, L.B.; Liao, Y.; Bai, R.H.; Shangguan, Z.P.; Deng, L. Divergent responses of autotrophic and heterotrophic respiration to nitrogen application in a *Pinus tabulaeformis* plantation. *Land Degrad. Dev.* **2025**, *36*, 5109–5121. [CrossRef]
5. Wu, X.Y.; Liu, Y.Y.; Zhang, H.J.; Dong, L.Z.; Zuo, Y.P.; Li, X.Y.; Wang, W. 12-year N addition enhances soil organic carbon decomposition by mediating microbial community composition in temperate plantations. *Appl. Soil Ecol.* **2025**, *206*, 105856. [CrossRef]
6. Xu, X.K.; Yue, J.; Cheng, W.G.; Kong, Y.H.; Tang, S.R.; Khoroshaev, D.; Shanin, V. Inhibition by nitrogen addition of moss-mediated CH_4 uptake and CO_2 emission under a well-drained temperate forest, northeastern China. *Plants* **2026**, *15*, 166. [CrossRef] [PubMed]
7. Xu, S.Q.; Chen, Z.M.; Zhang, N.; Li, Y.; Xu, Y.H.; Ding, W.X. Soil carbon quality determined the responses of respiration components to nitrogen fertilization and straw return. *Soil Till. Res.* **2026**, *259*, 107072. [CrossRef]
8. He, Y.L.; Qi, Y.C.; Peng, Q.; Dong, Y.S.; Yan, Z.Q.; Li, Z.L. Effects of exogenous carbon and nitrogen addition on the key process of carbon cycle in grassland ecosystem: A review. *China Environ. Sci.* **2018**, *38*, 1133–1141.
9. Cen, X.; Vitousek, P.; He, N.P.; Bond-lamberty, B.; Niu, S.L.; Du, E.Z.; Yu, K.L.; Zheng, M.H.; Sundert, K.V.; Paulus, E.L.; et al. A general framework for nitrogen deposition effects on soil respiration in global forests. *Nat. Commun.* **2025**, *17*, 506. [CrossRef] [PubMed]
10. Yakir, D.; Sternberg, L.S.L. The use of stable isotopes to study ecosystem gas exchange. *Oecologia* **2000**, *123*, 297–311. [CrossRef] [PubMed]
11. Kuzyakov, Y. Sources of CO_2 efflux from soil and review of partitioning methods. *Soil Biol. Biochem.* **2006**, *38*, 425–448. [CrossRef]
12. Millard, P.; Midwood, A.J.; Hunt, J.E.; Barbour, M.M.; Whitehead, D. Quantifying the contribution of soil organic matter turnover to forest soil respiration, using natural abundance $\delta^{13}C$. *Soil Biol. Biochem.* **2010**, *42*, 935–943. [CrossRef]
13. Moyes, A.B.; Gaines, S.J.; Siegwolf, R.T.W.; Bowling, D.R. Diffusive fractionation complicates isotopic partitioning of autotrophic and heterotrophic sources of soil respiration. *Plant Cell Environ.* **2010**, *33*, 1804–1819. [CrossRef] [PubMed]
14. Whitman, T.; Lehmann, J. A dual-isotope approach to allow conclusive partitioning between three sources. *Nat. Commun.* **2015**, *6*, 8708. [CrossRef] [PubMed]
15. Farquhar, G.D.; Lloyd, J.; Taylor, J.A.; Flanagan, L.B.; Syversten, J.P.; Hubick, K.T.; Wong, S.C.; Ehleringer, J.R. Vegetation effects on the isotopic composition of oxygen in atmospheric CO_2. *Nature* **1993**, *363*, 439–443. [CrossRef]
16. Ciais, P.; Tans, P.P.; Trolier, M.; White, J.W.C.; Francey, R.J. A large northern hemisphere terrestrial CO_2 sink indicated by the $^{13}C/^{12}C$ ratio of atmospheric CO_2. *Science* **1995**, *269*, 1098–1102. [CrossRef] [PubMed]
17. Ehleringer, J.R.; Bowling, D.R.; Flanagan, L.B.; Fessenden, J.; Helliker, B.; Martinelli, L.A.; Ometto, J.P. Stable isotopes and carbon cycle processes in forests and grasslands. *Plant Biol.* **2002**, *4*, 181–189. [CrossRef]
18. Bowling, D.R.; Pataki, D.E.; Randerson, J.T. Carbon isotopes in terrestrial ecosystem pools and CO_2 fluxes. *New Phytol.* **2008**, *178*, 24–40. [CrossRef] [PubMed]
19. Barbour, M.M.; Hunt, J.E.; Kodama, N.; Laubach, J.; McSeveny, T.M.; Rogers, G.N.D.; Tcherkez, G.; Wingate, L. Rapid changes in $\delta^{13}C$ of ecosystem-respired CO_2 after sunset are consistent with transient ^{13}C enrichment of leaf respired CO_2. *New Phytol.* **2011**, *190*, 990–1002. [CrossRef] [PubMed]
20. Miller, J.B.; Yakir, D.; White, J.W.C.; Tans, P.P. Measurement of $^{18}O/^{16}O$ in the soil-atmosphere CO_2 flux. *Glob. Biogeochem. Cycles* **1999**, *13*, 761–774. [CrossRef]
21. Riley, W.J.; Still, C.J.; Helliker, B.R.; Ribas-Carbo, M.; Berry, J.A. ^{18}O composition of CO_2 and H_2O ecosystem pools and fluxes in a tallgrass prairie: Simulations and comparisons to measurements. *Glob. Change Biol.* **2003**, *9*, 1567–1581. [CrossRef]
22. Wingate, L.; Ogée, J.; Cuntz, M.; Genty, B.; Reiter, L.; Seibt, U.; Yakir, D.; Maseyk, K.; Pendall, E.G.; Barbour, M.M.; et al. The impact of soil microorganisms on the global budget of $\delta^{18}O$ in atmospheric CO_2. *Proc. Natl. Acad. Sci. USA* **2009**, *106*, 22411–22415. [CrossRef] [PubMed]
23. Flanagan, L.B.; Brooks, J.R.; Varney, G.T.; Ehleringer, J.R. Discrimination against $C^{18}O^{16}O$ during photosynthesis and the oxygen isotope ratio of respired CO_2 in boreal forest ecosystems. *Glob. Biogeochem. Cycles* **1997**, *11*, 83–98. [CrossRef]
24. Flanagan, L.B.; Kubien, D.S.; Ehleringer, J.R. Spatial and temporal variation in the carbon and oxygen stable isotope ratio of respired CO_2 in a boreal forest ecosystem. *Tellus B Chem. Phys. Meteorol.* **1999**, *51*, 367–384. [CrossRef]
25. Wingate, L.; Ogée, J.; Burlett, R.; Bosc, A. Strong seasonal disequilibrium measured between the oxygen isotope signals of leaf and soil CO_2 exchange. *Glob. Change Biol.* **2010**, *16*, 3048–3064. [CrossRef]
26. Huang, X.M.; Terrer, C.; Dijkstra, F.A.; Hungate, B.A.; Zhang, W.J.; van Groenigen, K.J. New soil carbon sequestration with nitrogen enrichment: A meta-analysis. *Plant Soil* **2020**, *454*, 299–310. [CrossRef]
27. Ngaba, M.J.Y.; Uwiragiye, Y.; Bol, R.; Vries, W.D.; Zhou, J.B. Low-level nitrogen and short-term addition increase soil carbon sequestration in Chinese forest ecosystems. *Catena* **2022**, *215*, 106333. [CrossRef]

28. Hu, J.; Huang, C.; Zhou, S.; Kuzyakov, Y. Nitrogen deposition affects microbial carbon use efficiency: Meta-analysis of similarities and differences in ^{18}O and ^{13}C approaches. *Glob. Change Biol.* **2022**, *28*, 4977–4988. [CrossRef] [PubMed]
29. Min, K.; Billings, S.A. Microbes alter substrate from mineral-associated carbon to litterfall with nitrogen additions and warming. *Eur. J. Soil Sci.* **2024**, *75*, e13487. [CrossRef]
30. Xu, X.K.; Kong, Y.H.; Feng, E.P.; Yue, J.; Cheng, W.G.; Khoroshaev, D.; Kivalov, S. Effect of mosses and long-term N addition on $\delta^{13}C$ and $\delta^{18}O$ values of respired CO_2 under a temperate forest floor. *Plants* **2025**, *14*, 2707. [CrossRef] [PubMed]
31. Minich, L.I.; Geissbühler, D.; Tobler, S.; Udke, A.; Brunmayr, A.S.; Duborgel, M.M.; McMackin, C.; Wacker, L.; Gautschi, P.; Haghipour, N.; et al. Conceptualising carbon cycling pathways across different land-use types based on rates and ages of soil-respired CO_2. *Biogeosciences* **2026**, *23*, 811–829. [CrossRef]
32. Shim, J.H.; Pendall, E.; Morgan, J.A.; Ojima, D.S. Wetting and drying cycles drive variations in the stable carbon isotope ratio of respired carbon dioxide in semi-arid grassland. *Oecologia* **2009**, *160*, 321–333. [CrossRef] [PubMed]
33. Wynn, J.G.; Bird, M.I.; Wong, V.N.L. Rayleigh distillation and the depth profile of $^{13}C/^{12}C$ ratios of soil organic carbon from soils of disparate texture in Iron Range National Park, Far North Queensland, Australia. *Geochim. Cosmochim. Acta* **2005**, *69*, 1961–1973. [CrossRef]
34. Von Sperber, C.; Weiler, M.; Brüggemann, N. The effect of soil moisture, soil particle size, litter layer and carbonic anhydrase on the oxygen isotopic composition of soil-released CO_2. *Eur. J. Soil Sci.* **2015**, *66*, 566–576. [CrossRef]
35. Pries, C.H.; Angert, A.; Castanha, C.; Hilman, B.; Torn, M.S. Using respiration quotients to track changing sources of soil respiration seasonally and with experimental warming. *Biogeosciences* **2020**, *17*, 3045–3055. [CrossRef]
36. Kato, T.; Nakazawa, T.; Aoki, S.; Sugawara, S.; Ishizawa, M. Seasonal variation of the oxygen isotopic ratio of atmospheric carbon dioxide in a temperate forest, Japan. *Glob. Biogeochem. Cycles* **2004**, *18*, GB2003. [CrossRef]
37. Billings, S.A.; Brecheisen, Z.; Cherkinsky, A.; Lehmeier, C.; Cook, C.W.; Markewitz, D.; Souza, L.F.T.; Reuman, D.; Richter, D.D. Persistent biogeochemical signals of land use-driven, deep root losses illuminated by C and O isotopes of soil CO_2 and O_2. *Biogeochemistry* **2024**, *167*, 1469–1489. [CrossRef]
38. Diao, H.Y.; Wang, A.Z.; Yuan, F.H.; Guan, D.X.; Wu, J.B. Autotrophic respiration modulates the carbon isotope composition of soil respiration in a mixed forest. *Sci. Total Environ.* **2022**, *807*, 150834. [CrossRef] [PubMed]
39. Xu, X.K.; Wu, H.H.; Yue, J.; Tang, S.R.; Cheng, W.G. Effects of snow cover on carbon dioxide emissions and their $\delta^{13}C$ values of temperate forest soils with and without litter. *Forests* **2023**, *14*, 1384. [CrossRef]
40. Fessenden, J.E.; Ehleringer, J.R. Temporal variation in $\delta^{13}C$ of ecosystem respiration in the Pacific Northwest: Links to moisture stress. *Oecologia* **2003**, *136*, 129–136. [CrossRef] [PubMed]
41. Pataki, D.E.; Ehleringer, J.R.; Flanagan, L.B.; Yakir, D.; Bowling, D.R.; Still, C.J.; Buchmann, N.; Kaplan, J.O.; Berry, J.A. The application and interpretation of Keeling plots in terrestrial carbon cycle research. *Glob. Biogeochem. Cycles* **2003**, *17*, 1022. [CrossRef]
42. Ometto, J.P.H.; Flanagan, L.B.; Martinelli, L.A.; Ehleringer, J.R. Oxygen isotope ratios of waters and respired CO_2 in Amozonian forest and pasture ecosystems. *Ecol. Appl.* **2005**, *15*, 58–70. [CrossRef]
43. Xu, X.K.; Han, L.; Luo, X.B.; Han, S.J. Synergistic effects of nitrogen amendments and ethylene on atmospheric methane uptake under a temperate old-growth forest. *Adv. Atmos. Sci.* **2011**, *28*, 843–854. [CrossRef]
44. Xia, N.; Du, E.Z.; Wu, X.H.; Tang, Y.; Wang, Y.; de Vries, W. Effects of nitrogen addition on soil methane uptake in global forest biomes. *Environ. Pollut.* **2020**, *264*, 114751. [CrossRef] [PubMed]
45. Xu, X.K.; Inubushi, K. Effects of N sources and methane concentrations on methane uptake potential of a typical coniferous forest and its adjacent orchard soil. *Biol. Fertil. Soils* **2004**, *40*, 215–221. [CrossRef]
46. Xu, X.K.; Inubushi, K. Responses of ethylene and methane consumption to temperature and pH in temperate volcanic forest soils. *Eur. J. Soil Sci.* **2009**, *60*, 489–498. [CrossRef]
47. Jordan, S.F.A.; Schloemer, S.; Krüger, M.; Heffner, T.; Horn, M.A.; Blumenberg, M. Interferences caused by the biogeochemical methane cycle in peats during the assessment of abandoned oil wells. *Biogeosciences* **2025**, *22*, 809–830. [CrossRef]
48. Wu, H.H.; Xu, X.K.; Duan, C.T.; Li, T.S.; Cheng, W.G. Synergistic effects of dissolved organic carbon and inorganic nitrogen on methane uptake in forest soils without and with freezing treatment. *Sci. Rep.* **2016**, *6*, 32555. [CrossRef] [PubMed]
49. Kammer, A.; Tuzson, B.; Emmenegger, L.; Knohl, A.; Mohn, J.; Hagedorn, F. Application of a quantum cascade laser-based spectrometer in a closed chamber system for real-time $\delta^{13}C$ and $\delta^{18}O$ measurements of soil-respired CO_2. *Agric. For. Meteorol.* **2011**, *151*, 39–48. [CrossRef]
50. Xu, X.K.; Xu, T.T.; Yue, J. Effect of in situ large soil column translocation on CO_2 and CH_4 fluxes under two temperate forests of northeastern China. *Forests* **2023**, *14*, 1531. [CrossRef]
51. Keeling, C.D. The concentration and isotopic abundances of atmospheric carbon dioxide in rural areas. *Geochim. Cosmochim. Acta* **1958**, *13*, 322–334. [CrossRef]
52. Keeling, C.D. The concentration and isotopic abundances of carbon dioxide in rural and marine air. *Geochim. Cosmochim. Acta* **1961**, *24*, 277–298. [CrossRef]

53. Nottingham, A.T.; Turner, B.L.; Chamberlain, P.M.; Stott, A.W.; Tanner, E.V.J. Priming and microbial nutrient limitation in lowland tropical forest soils of contrasting fertility. *Biogeochemistry* **2012**, *111*, 219–237. [CrossRef]
54. Gavrichkova, O.; Proietti, S.; Moscatello, S.; Portarena, S.; Battistelli, A.; Matteucci, G.; Brugnoli, E. Short-term natural $\delta^{13}C$ and $\delta^{18}O$ variations in pools and fluxes in a beech forest: The transfer of isotopic signal from recent photosynthates to soil respired CO_2. *Biogeosciences* **2011**, *8*, 2833–2846. [CrossRef]
55. Werner, C.; Schnyder, H.; Cuntz, M.; Keitel, C.; Zeeman, M.J.; Dawson, T.E.; Badeck, F.W.; Brugnoli, E.; Ghashghaie, J.; Grams, T.E.E.; et al. Progress and challenges in using stable isotopes to trace plant carbon and water relations across scales. *Biogeosciences* **2012**, *9*, 3083–3111. [CrossRef]
56. Min, K.; Lehmeier, C.A.; Ballantyne, F.; Billings, S.A. Carbon availability modifies temperature responses of heterotrophic microbial respiration, carbon uptake affinity, and stable carbon isotope discrimination. *Front. Microbiol.* **2016**, *7*, 2083. [CrossRef] [PubMed]
57. Hicks, L.C.; Meir, P.; Nottingham, A.; Reay, D.; Stott, A.W.; Salinas, N.; Whitaker, J. Carbon and nitrogen inputs differentially affect priming of soil organic matter in tropical lowland and montane soils. *Soil Biol. Biochem.* **2019**, *129*, 212–222. [CrossRef]
58. Kapiluto, Y.; Yakir, D.; Tans, P.; Berkowitz, B. Experimental and numerical studies of the ^{18}O exchange between CO_2 and water in the atmosphere–soil invasion flux. *Geochim. Cosmochim. Acta* **2007**, *71*, 2657–2671. [CrossRef]
59. Seibt, U.; Wingate, L.; Lloyd, J.; Berry, J.A. Diurnally variable $\delta^{18}O$ signatures of soil CO_2 fluxes indicate carbonic anhydrase activity in a forest soil. *J. Geophys. Res.* **2006**, *111*, G04005. [CrossRef]
60. Volk, M.; Bassin, S.; Lehmann, M.F.; Johnson, M.G.; Andersen, C.P. ^{13}C isotopic signature and C concentration of soil density fractions illustrate reduced C allocation to subalpine grassland soil under high atmospheric N deposition. *Soil Biol. Biochem.* **2018**, *125*, 178–184. [CrossRef] [PubMed]
61. Li, Y.; Liu, Y.H.; Wu, S.M.; Nie, C.; Lorenz, N.; Lee, N.R.; Dick, R.P. Composition and carbon utilization of soil microbial communities subjected to long-term nitrogen fertilization in a temperate grassland in northern China. *Appl. Soil Ecol.* **2018**, *124*, 252–261. [CrossRef]
62. Eberwein, J.R.; Oikawa, P.Y.; Allsman, L.A.; Jenerette, G.D. Carbon availability regulates soil respiration response to nitrogen and temperature. *Soil Biol. Biochem.* **2015**, *88*, 158–164. [CrossRef]
63. Zakharova, A.; Beare, M.H.; Cieraad, E.; Curtin, D.; Turnbull, M.H.; Millard, P. Factors controlling labile soil organic matter vulnerability to loss following disturbance as assessed by measurement of soil-respired $\delta^{13}CO_2$. *Eur. J. Soil Sci.* **2015**, *66*, 135–144. [CrossRef]
64. Delancey, L.C.; Zhao, Q.; Keller, A.B.; Walter, C.A.; Hofmockel, K.S.; Mayes, M.A.; Seabloom, E.W.; Borer, E.T.; Leakey, A.D.B.; Hobbie, S.E. Carbon availability, soil pH, and microbial allocation to nitrogen acquisition shape grassland heterotrophic respiration in response to a decade of nitrogen addition. *Soil Biol. Biochem.* **2026**, *212*, 110000. [CrossRef]
65. Lai, C.T.; Riley, W.; Owensby, C.; Ham, J.; Schauer, A.; Ehleringer, J.R. Seasonal and interannual variations of carbon and oxygen isotopes of respired CO_2 in a tallgrass prairie: Measurements and modeling results from 3 years with contrasting water availability. *J. Geophys. Res.* **2006**, *11*, D08S06. [CrossRef]
66. Takahashi, Y.; Liang, N.S.; Hirata, R.; Machida, T.; Fujinuma, Y. Variability in carbon stable isotope ratio of heterotrophic respiration in a deciduous needle-leaf forest. *J. Geophys. Res. Biogeosci.* **2008**, *113*, G01022. [CrossRef]
67. Formánek, P.; Ambus, P. Assessing the use of $\delta^{13}C$ natural abundance in separation of root and microbial respiration in a Danish beech (*Fagus sylvatica* L.) forest. *Rapid Commun. Mass Spectrom.* **2004**, *18*, 615–621. [CrossRef] [PubMed]
68. Ekblad, A.; Högberg, P. Natural abundance of ^{13}C in CO_2 respired from forest soils reveals speed of link between tree photosynthesis and root respiration. *Oecologia* **2001**, *127*, 305–308. [CrossRef] [PubMed]
69. Andrews, J.A.; Matamala, R.; Westover, K.M.; Schlesinger, W.H. Temperature effects on the diversity of soil heterotrophs and the $\delta^{13}C$ of soil-respired CO_2. *Soil Biol. Biochem.* **2000**, *32*, 699–706. [CrossRef]
70. Siegwolf, R.T.W.; Lehmann, M.M.; Goldsmith, G.R.; Churakova, O.V.; Olga, V.; Mirande-Ney, C.; Timoveeva, G.; Weigt, R.B.; Saurer, M. Updating the dual C and O isotope-gas-exchange model: A concept to understand plant responses to the environment and its implications for tree rings. *New Phytol.* **2020**, *226*, 1550. [CrossRef] [PubMed]
71. Xu, X.K.; Duan, C.T.; Wu, H.H.; Luo, X.B.; Han, L. Effects of changes in throughfall on soil GHG fluxes under a mature temperate forest, northeastern China. *J. Environ. Manag.* **2021**, *294*, 112950. [CrossRef] [PubMed]
72. Stern, L.; Baisden, W.T.; Amundson, R. Processes controlling the oxygen isotope ratio of soil CO_2: Analytic and numerical modeling. *Geochim. Cosmochim. Acta* **1999**, *63*, 799–814. [CrossRef]
73. Wang, J.Y.; Wang, X.J.; Wang, J.P.; Lu, T.P. Dynamics of soil CO_2 and CO_2 efflux in arid soil. In *Carbon Cycle in the Changing Arid Land of China*; Wang, X.J., Yu, Z.T., Wang, J.P., Zhang, J., Eds.; Springer: Singapore, 2018; pp. 55–68. [CrossRef]
74. Mortazavi, B.; Prater, J.L.; Chanton, J.P. A field-based method for simultaneous measurements of the $\delta^{18}O$ and $\delta^{13}C$ of soil CO_2 efflux. *Biogeosciences* **2004**, *1*, 1–9. [CrossRef]

75. Riley, W.J.; Still, C.J.; Torn, M.S.; Berry, J.A. A mechanistic model of $H_2{}^{18}O$ and $C^{18}OO$ fluxes between ecosystems and the atmosphere: Model description and sensitivity analyses. *Glob. Biogeochem. Cycles* **2002**, *16*, 1095. [CrossRef]
76. Aranibar, J.N.; Berry, J.A.; Riley, W.J.; Pataki, D.E.; Law, B.E.; Ehleringer, J.R. Combining meteorology, eddy fluxes, isotope measurements, and modeling to understand environmental controls of carbon isotope discrimination at the canopy scale. *Glob. Change Biol.* **2006**, *12*, 710–730. [CrossRef]

Disclaimer/Publisher's Note: The statements, opinions and data contained in all publications are solely those of the individual author(s) and contributor(s) and not of MDPI and/or the editor(s). MDPI and/or the editor(s) disclaim responsibility for any injury to people or property resulting from any ideas, methods, instructions or products referred to in the content.